Role of Oncostatin M in the Pathogenesis of Vernal Keratoconjunctivitis: Focus on the Barrier Function of the Epithelium and Interleukin-33 Production by Fibroblasts

Ishin Ninomiya,[1–3] Kenji Yamatoya,[3] Keitaro Mashimo,[2] Akira Matsuda,[4] Ayumi Usui-Ouchi,[2] Yoshihiko Araki,[3] and Nobuyuki Ebihara[2,3]

[1]Juntendo University Graduate School of Medicine, Tokyo, Japan
[2]Department of Ophthalmology, Juntendo University Urayasu Hospital, Chiba, Japan
[3]Institute for Environmental and Gender-Specific Medicine, Juntendo University Graduate School of Medicine, Chiba, Japan
[4]Department of Ophthalmology, Juntendo University School of Medicine, Tokyo, Japan

Correspondence: Nobuyuki Ebihara, Department of Ophthalmology, Juntendo University Urayasu Hospital 2-1-1, Tomioka Urayasu Chiba, Japan; ebihara@juntendo.ac.jp.

Received: August 16, 2022
Accepted: December 10, 2022
Published: December 29, 2022

Citation: Ninomiya I, Yamatoya K, Mashimo K, et al. Role of oncostatin M in the pathogenesis of vernal keratoconjunctivitis: Focus on the barrier function of the epithelium and interleukin-33 production by fibroblasts. *Invest Ophthalmol Vis Sci.* 2022;63(13):26. https://doi.org/10.1167/iovs.63.13.26

Purpose. Vernal keratoconjunctivitis (VKC) is a severe, recurrent allergic conjunctivitis. Previously, we found high concentrations of oncostatin M (OSM) in the tears of patients with VKC. Here, we investigated the role of OSM in VKC by focusing on epithelial barrier function and IL-33 production.

Methods. To assess the effect of OSM on the barrier function of human conjunctival epithelial cells (HConEpiCs), we measured transepithelial electrical resistance and dextran permeability. We also assessed expression of tight junction–related proteins such as E-cadherin and ZO-1 in HConEpiCs by Western blotting and immunofluorescence. Then we used immunohistochemistry to evaluate expression of Ki-67, E-cadherin, epithelial-mesenchymal transition–related proteins, and IL-33 in giant papillae (GPs) from patients with VKC. In addition, we used Western blotting, microarray, quantitative real-time polymerase chain reaction, and enzyme-linked immunosorbent assay to examine whether OSM activates signal transducer and activator of transcription 1 (STAT1) or STAT3 and induces the expression of various genes in human conjunctival fibroblasts (HConFs).

Results. OSM reduced expression of E-cadherin and ZO-1 in HConEpiCs, indicating barrier dysfunction. In immunohistochemistry, Ki-67 expression was present in the lower epithelial layer of the GPs, and E-cadherin expression was reduced in the superficial and lower layers; double staining revealed that GPs had a high number of fibroblasts expressing IL-33. In addition, in HConFs, OSM phosphorylated both STAT1 and STAT3 and induced IL-33.

Conclusions. OSM has important roles in severe, prolonged allergic inflammation by inducing epithelial barrier dysfunction and IL-33 production by conjunctival fibroblasts.

Keywords: vernal keratoconjunctivitis, allergic inflammation, conjunctival fibroblasts

Oncostatin M (OSM) is a member of the IL-6 cytokine family, which includes IL-6, IL-11, leukemia inhibitory factor (LIF), and cardiotrophin-1. OSM is produced primarily by activated T cells, monocytes, dendritic cells, mast cells, and neutrophils, and its amino acid sequence identity to LIF is 27%.[1–6] Two different OSM receptors (OSMRs) have been discovered so far: OSMR type I, which consists of the LIF receptor (LIFR)/gp130, and OSMR type II, which consists of OSMRβ/gp130. Binding of ligands to these receptor complexes activates various signaling cascades, including the Janus kinase/signal transducer and activator of transcription (JAK/STAT) and mitogen-activated protein kinase pathways.[7,8] Although gp130 is ubiquitously expressed, the specific OSMR subunits, LIFR and OSMRβ, are restricted to certain tissues, including the kidney, pancreas, liver, and lung. OSM is a member of the gp130 family of cytokines, which are involved in homeostasis and diseases associated with chronic inflammation.[1,9] It has pleiotropic functions in differentiation, cell proliferation, fibrosis, and epithelial-mesenchymal transition (EMT).[8,10–15] In a previous study, we detected high concentrations of OSM in the tears of patients with vernal keratoconjunctivitis (VKC).[16]

Recently, several reports have shown that OSM promotes epithelial and endothelial barrier dysfunction.[17–21] By using transepithelial electrical resistance (TEER), Takata et al.[17] demonstrated that OSM impaired the barrier function of rat brain endothelial cell monolayers and decreased the expression of tight junction–related proteins, such as E-cadherin and occludin. Pothoven et al.[18] also detected excessive OSM expression in nasal polyps of patients with severe eosinophilic rhinitis and showed that OSM reduced occludin expression in cultured human bronchial epithelial cells, resulting in epithelial barrier dysfunction.

Epithelial barrier dysfunction may induce type 2 immunity and the development of allergies. For example, several reports have shown that excessive OSM expression is sufficient to induce a type 2 immune response in the lung and nose.[18,22–24] In addition, some reports showed that IL-33 induced a severe allergic reaction via type 2 immunity.[25] IL-33 belongs to the damage-associated molecular patterns (DAMPs) and is released by cell injury. In VKC giant papillae (GPs), abundant IL-33 was observed in the nucleus of epithelial cells and vascular endothelial cells.[26] IL-33 is produced by fibroblasts, among other cells; however, the production mechanism is unclear.

Epithelial cell barrier dysfunction may cause an excessive allergic reaction in GPs of patients with VKC, and in this study, we evaluated whether OSM contributes to epithelial barrier dysfunction in cultured human conjunctival epithelial cells (HConEpiCs). We also focused on IL-33 production by fibroblasts as an important factor in excessive allergic reactions and investigated the involvement of OSM.

Materials and Methods

Materials

The necessary materials were purchased as follows: human recombinant OSM was purchased from Proteintech Group Inc. (Rosemont, IL, USA); mouse monoclonal antibodies, including anti–ZO-1 IgG_1 (#33-9100), anti–E-cadherin IgG_1 (#13-1700), anti-occludin $IgG_{1\kappa}$ (#33-1500), anti-STAT1 $IgG_{1\kappa}$ (#AHO0832), anti–phospho-STAT1 (anti-pSTAT1) $IgG_{2a\kappa}$ (#33-3400), anti-STAT3 IgG_{2a} (#MA1-13042), anti–phospho-STAT3 (anti-pSTAT3) IgG_1 (#MA5-15193), and Alexa Flour 488–conjugated goat anti-mouse IgG_1, from Thermo Fisher Scientific, Inc. (Waltham, MA, USA); mouse monoclonal anti-OSMRβ monoclonal $IgG_{1\kappa}$, from Santa Cruz Biotechnology (Dallas, TX, USA); rabbit anti–Ki-67, mouse anti–E-cadherin, rabbit anti-vimentin, rabbit anti-S100A4, mouse anti–α-smooth muscle actin (α-SMA), rabbit anti–N-cadherin, rabbit anti–IL-33, and mouse anti–human-fibroblast antibodies, from Abcam (Cambridge, UK); affinity purified goat anti–IL-33 polyclonal antibody, from R&D Biosystems; mouse anti–human fibroblast monoclonal antibody, from Millipore-Chemicon (Temecula, CA, USA); and horseradish peroxidase–coupled anti-mouse IgG, from Dako Inc. (Carpinteria, CA, USA).

Human Samples

After obtaining written informed consent from participants, GPs were resected for therapeutic purposes from four patients with VKC, and control conjunctival tissue was biopsied from eight patients with conjunctivochalasis during resection surgery. Samples of conjunctivochalasis were a generous gift from Dr. Norihiko Yokoi (Department of Ophthalmology, Kyoto Prefectural University of Medicine). All procedures were approved by the ethics committees of Juntendo University School of Medicine (approval No. 2019244) and Kyoto Prefectural University of Medicine, and the study was conducted in accordance with the tenets of the Declaration of Helsinki.

Immunohistochemistry

The tissue sections were fixed in formalin and embedded in paraffin. Immunohistochemical studies were performed on 7-µm serial tissue sections. After deparaffinization and rehydration, all the sections were blocked by 2% BSA at room temperature (RT) for 1 hour.

For single immunostaining, the sections were incubated overnight at 4°C with the abovementioned antibodies (i.e., mouse monoclonal antibodies, rabbit anti–Ki-67, mouse anti–E-cadherin, rabbit antivimentin, rabbit anti-S100A4, mouse anti–α-SMA, and rabbit anti–N-cadherin). Slides were washed twice in Tris-buffered saline with 0.1% Tween 20, incubated for 45 minutes in each of the biotinylated second antibodies in PBS, washed twice, and then incubated with Vectastain Elite ABC Reagent (Vector Laboratories, Burlingame, CA, USA) for 45 minutes and washed twice. Signals were developed with 3,3′-diaminobenzidine for 10 minutes at RT. Slides were counterstained with hematoxylin.

For double immunohistochemical staining, the sections were incubated simultaneously with anti–IL-33 (1:100) or anti–fibroblast antibody (1:100) and incubated overnight at 4°C. Then, the slides were washed in PBS and incubated with a mixture of Alexa 594–conjugated donkey anti–goat-IgG and Alexa 488–conjugated donkey anti–mouse-IgG (both 1:1000, multiple staining grade, obtained from Invitrogen, Carlsbad, CA, USA) for 1 hour at RT. Finally, the slides were mounted with Vectashield with 4′,6-diamidino-2-phenylindole (DAPI; Vector Laboratories), and the specimens were examined with a confocal laser-scanning microscope (FV-1000; Olympus, Tokyo, Japan).

Cell Culture

HConEpiCs were a generous gift from Dr. Satoshi Kawasaki (Department of Ophthalmology, Osaka University, Japan).[27–29] Primary cultured human conjunctival fibroblasts (HConFs) were purchased from ScienCell Research Laboratories (Carlsbad, CA, USA). HConEpiCs were cultured in keratinocyte serum-free medium (#17005042; Thermo Fisher Scientific, Inc.) supplemented with attached 25-mg bovine pituitary extract and 2.5-µg epithelial growth factor. HConFs were cultured in Dulbecco's modified Eagle's medium (DMEM) supplemented with 10% (v/v) fetal bovine serum (FBS). Both mediums were supplemented with 100 U/mL penicillin and 100 µg/mL streptomycin (Sigma-Aldrich, St. Louis, MO, USA). Cells were cultured in a CO_2 incubator (37°C, 5% CO_2) and passaged at 70% to 80% confluency by using trypsin 0.025% (w/v)/EDTA 0.01% (w/v) (Kurabo Industries Ltd., Osaka, Japan).

Epithelial Permeability Assay

Barrier function was measured by two methods: TEER and FITC-labeled dextran permeability. HConEpiCs were seeded at a density of 1.0×10^5 cells/mL (500 µL) on the apical chamber of a Transwell polyester membrane insert (#3460, 0.4-µm pore size, 12-mm diameter; Corning Inc., Corning, NY, USA). TEER was measured with a Millicell ERS-2 volt-ohm meter (Millipore Corp, Burlington, MA, USA) equipped with an STX01 electrode (World Precision Instruments, Sarasota, FL, USA). After cells reached confluent monolayers and showed steady resistance values, the whole medium was changed for medium containing OSM (0, 1, 10, and 100 ng/mL). Resistance values were recorded at 48 hours after stimulation and calculated by subtracting the blank resistance, and the values were revised by the effective growth area of the membrane (1.12 cm^2), according to the manufacturer's instructions. Next, epithelial permeability across

Investigative Ophthalmology & Visual Science

Table. Primers Used for Quantitative PCR

Gene	Primer Combination
SOCS3 forward	5′-CATCTCTGTCGGAAGTCA-3′
SOCS3 reverse	5′-GCATCGTACTGGTCCAGGAACT-3′
SERPINβ3 forward	5′-TTACCTCGGTTCAAAGTGGAAGAG-3′
SERPINβ3 reverse	5′-AATCCTACTACAGCGGTGGCAG-3′
IL-33 forward	5′-GCCTGTCAACAGCAGTCTACTG-3′
IL-33 reverse	5′-TGTGCTTAGAGAAGCAAGATACTC-3′
CCL8 forward	5′-GGGTGCTGAAAAGCTACGAGAG-3′
CCL8 reverse	5′-GGATCTCCATGTACTCACTGACC-3′
VEGFA forward	5′-TTGCCTTGCTGCTCTACCTCCA-3′
VEGFA reverse	5′-GATGGCAGTAGCTGCGCTGATA-3′

the HConEpiC monolayer was assessed by measuring the paracellular flux of FITC-labeled dextran (FD10; 10 kDa, 1 mg/mL; Sigma-Aldrich) from the apical chambers to the basolateral chambers. The FD10 solution was added to the apical chamber (500 µL), and 1500 µL of the medium without FD10 was added to the basolateral chamber. Cells were incubated at 37°C for 30 minutes. Then, the apical chambers were removed and the fluorescence intensity of the solution in the basolateral chambers was measured by ARVO X4 (Perkin Elmer, Waltham, MA, USA).

Immunocytochemistry

HConEpiCs were seeded in a LAB-TEK chamber slide system (4 wells; Thermo Fisher Scientific) at 0.5×10^5 cells/well. The culture medium was changed every day for at least 10 days. Then, after full confluency was reached, cells were exposed to OSM solution (0, 1, 10, and 100 ng/mL) for 48 hours. Cells on slides were fixed with 4% paraformaldehyde diluted in PBS for 5 minutes, permeabilized in 0.1% Triton X-100 diluted in PBS for 10 minutes at RT, and blocked with 1% BSA in PBS containing 0.1% Tween 20 (PBST) for 1 hour at RT. Then, after washing twice with PBST for 5 minutes each, slides were incubated with anti–E-cadherin (1 µg/mL) or anti–ZO-1 (5 µg/mL) antibodies for 1 hour at RT. After washing three times with PBST for 5 minutes each, slides were subsequently incubated with secondary antibody (goat anti-mouse IgG_1 Alexa Flour 488, 1:2000) for 1 hour at RT and washed three times with PBST for 5 minutes each. Slides were counterstained and mounted with Vectashield antifade with a DAPI mounting medium (Vector Laboratories). HConFs were used before confluence and stained with anti-OSMRβ antibody (2 µg/mL) by almost the same method. BZ-X810 (Keyence, Osaka, Japan) equipped with a Plan Apo Lambda 40XC/0.95NA objective lens (Nikon, Tokyo, Japan) was used for observation.

Western Blotting

HConEpiCs and HConFs were cultured in a 6-well plate until confluence and stimulated by OSM (0, 1, 10, and 100 ng/mL) for 10 minutes (HConFs) or 48 hours (HConEpiCs). Proteins were extracted in cell lysis buffer (50 mM Tris-HCl buffer, 0.15 M NaCl, 0.1% sodium dodecyl sulfate, 1% Triton X-100, 1% sodium deoxycholate, and cOmplete protease inhibitor cocktail (Roche, Basel, Switzerland) for 15 minutes at 4°C. Then, cell lysates were centrifuged at 15,000 rpm for 10 minutes, and the supernatant was used as the samples for the experiments. After samples were quantified and equalized by the Bradford method, they were subjected to sodium dodecyl sulfate–polyacrylamide gel electrophoresis, transferred to polyvinylidene difluoride membranes, and examined by immunoblot analysis. Membranes were blocked with 1% skim milk diluted in PBST and incubated overnight at 4°C with anti–E-cadherin (2 µg/mL), anti–ZO-1 (2.5 µg/mL), anti-STAT1 (1:500), anti-pSTAT1 (1 µg/mL), anti-STAT3 (2 µg/mL), anti-pSTAT3 (2 µg/mL), or anti–β-actin (Sigma-Aldrich) antibodies. Horseradish peroxidase–coupled anti-mouse IgG (0.65 µg/mL; Dako Inc.) was used as the secondary antibody. Immunoreactive bands were visualized by Amersham ECL Prime and observed by Amersham Imager-600 (both from GE Healthcare Life Sciences, Chicago, IL, USA).

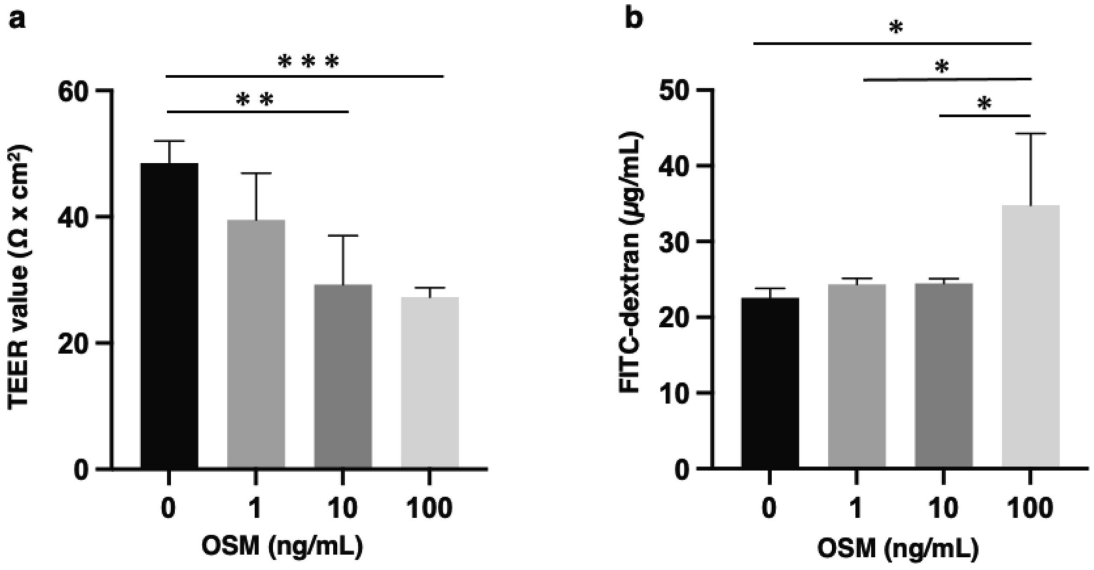

Figure 1. Effect of OSM on barrier function of human conjunctival epithelial cells. Transepithelial electrical resistance (**a**) and FITC-labeled dextran permeability (**b**) in monolayers of HConEpiCs treated with oncostatin M (0, 1, 10, 100 ng/mL). Data are representative mean ± SD values of four samples for each group (*$P < 0.05$, **$P < 0.01$, ***$P < 0.0001$, one-way ANOVA with Tukey test).

Investigative Ophthalmology & Visual Science

DNA Microarray Analysis

Before the following experiments, HConFs in the third passage were incubated in DMEM without FBS and growth supplements for 24 hours. Then, the cells were stimulated for 12 hours with 100 ng/mL OSM, and RNA was extracted with an RNeasy Mini Kit (QIAGEN, Hilden, Germany) according to the manufacturer's instructions. Gene expression microarray analysis, performed with the Human Gene 2.0 ST Array (Thermo Fisher Scientific), which contains 53,617 probes characterizing human genes, was consigned to Filgen Inc. (Nagoya, Japan). Predictive enrichment analysis was performed on sets of genes exhibiting an expression change (fold change >2, <0.5). Data are presented as a heatmap and MA (mean average) plots generated with MeV (http://mev.tm4.org) and Prism 8 software (GraphPad, La Jolla, CA, USA).

Quantitative Real-Time Polymerase Chain Reaction

Before the following experiments, HConFs were prepared as described above. Then, the cells were stimulated for 12 hours with 20 or 100 ng/mL OSM, and RNA was extracted with an RNeasy Mini Kit (QIAGEN) according to the manufacturer's instructions. Complementary DNA was synthesized from 750 ng total RNA by using PrimeScript RT Master Mix (Takara Bio Inc., Shiga, Japan). Quantitative real-time PCR was then performed with a SYBR Premix Ex Taq II (TliRNaseH Plus; Takara Bio Inc.) and an Applied Biosystems 7900HT thermocycler and analyzed by Sequence Detection System 2.4 (Applied Biosystems, Foster City, CA, USA). The primers used are shown in the Table. *GAPDH* was used as the reference gene.

Enzyme-Linked Immunosorbent Assay

Before the following experiments, HConFs were prepared as stated above. Then, the cells were stimulated with various concentrations of OSM for 24 hours. Cell lysates were obtained by exposing cells to cell lysis buffer for 15 minutes at 4°C and centrifuging the solution at 15,000 rpm for 10 minutes. Purified cell lysate was used for detecting intracellular IL-33 with an ELISA kit (#D3300B, #DVE00; R&D Systems, Minneapolis, MN, USA), according to the manufacturer's instructions.

Statistical Analysis

All results are expressed as the mean and SD. Analyses were performed with GraphPad Prism software (GraphPad). Data were compared between two groups by a two-tailed Student's *t*-test and between multiple groups by one-way ANOVA with a Tukey test. *P* values of less than 0.05 were considered statistically significant.

Results

Decreased Barrier Function in HConEpiCs Cultured With OSM

TEER and FITC-labeled dextran permeability were used to assay the barrier function of HConEpiCs under OSM stimulation. If a barrier is intact, TEER is high and dextran permeability is low, but OSM-stimulated HConEpiCs showed a

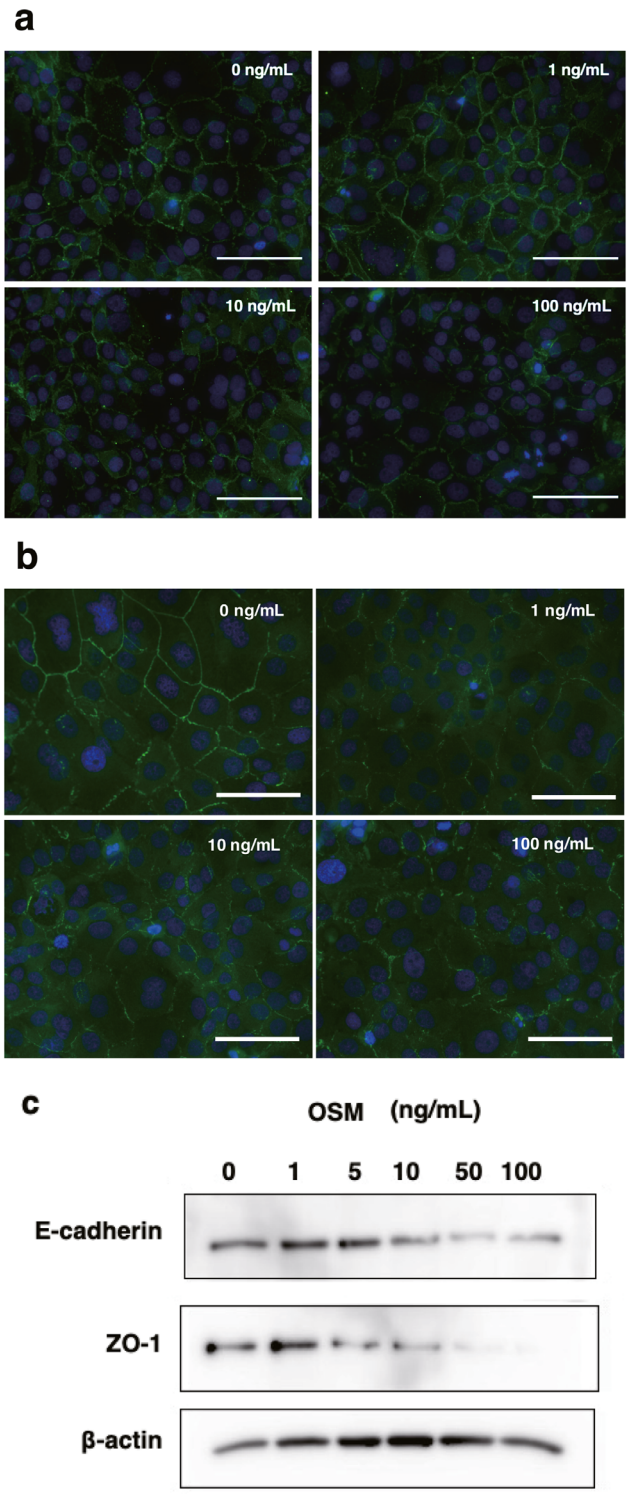

Figure 2. Effect of OSM on expression of tight junction proteins in human conjunctival epithelial cells. Expression of E-cadherin (**a**) and ZO-1 (**b**) in HConEpiCs treated with OSM (0, 1, 10, and 100 ng/mL), assessed by immunocytochemistry. *Bars*: 50 µm. Similarly, expression of E-cadherin and ZO-1 in HConEpiCs treated with OSM (0, 1, 5, 10, 50, and 100 ng/mL), assessed by Western blotting (**c**). Immunoreactive bands of *β*-actin (*lower row*) are shown as a control.

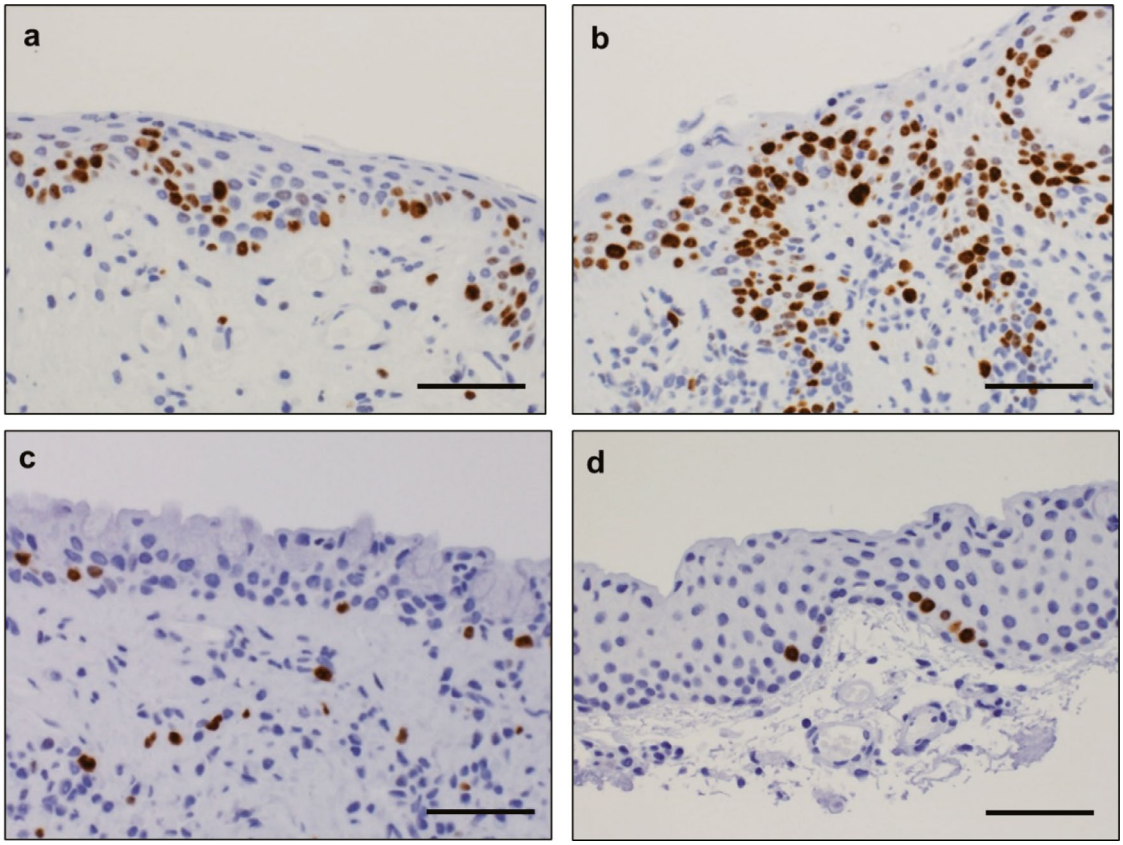

Figure 3. Expression of Ki-67 in the epithelium of giant papillae from patients with vernal keratoconjunctivitis and in control samples from patients with conjunctivochalasis. Immunoreactivity of Ki-67 of giant papillae in multilayer epithelium (**a**), invasive epithelium (**b**), well-differentiated epithelium (**c**), and control samples (**d**). Ki-67–positive cells stained by *brown* nuclear staining. *Bars*: 50 µm.

lower TEER value and higher dextran permeability than the vehicle-stimulated ones (Figs. 1a, 1b). OSM stimulation of HConEpiCs did not decrease their viability, as assessed by WST8 assay (data not shown).

Change in Expression of E-cadherin and ZO-1 by OSM

We investigated whether OSM altered the expression of E-cadherin and ZO-1 in vitro. In immunofluorescence, the characteristic lattice-like structure of E-cadherin and ZO-1 was seen in unstimulated HConEpiCs. However, the expression of both substances was reduced in HConEpiCs stimulated by OSM at 10 and 100 ng/mL (Figs. 2a, 2b). In Western blotting, E-cadherin and ZO-1 expression was reduced with same OSM concentrations (Fig. 2c).

Expression of Ki-67, E-cadherin, N-cadherin, Vimentin, S100A4, and α-SMA in Immunohistochemistry of VKC GPs

We performed immunohistochemistry to examine the characteristics of VKC GPs. Ki-67 was stained because conjunctival proliferative change is typical in VKC. Abundant Ki-67–positive cells were observed in the lower epithelial layer and in the invasive epithelium of GPs (Figs. 3a, 3b), but only a few Ki-67–positive cells were observed in the well-differentiated epithelium and in control samples (Figs. 3c, 3d).

Next, E-cadherin and mesenchymal molecules were stained to detect EMT. E-cadherin expression differed in various parts of the epithelium of VKC GPs: E-cadherin was expressed along the cell membrane in the middle layer, showed a cytoplasmic expression pattern in the lower layer, and was not expressed in the upper layer (Fig. 4a). In contrast, in control samples, strong expression was observed in all layers of the epithelium and along the cell membrane (Fig. 4b). Some expression of N-cadherin was observed in the cytoplasm of the GP epithelial cells. Vimentin was expressed in only a few epithelial cells. S100A4, the marker of fibroblasts, appeared almost exclusively in invasive epithelium and was abundant in the substantia propria. α-SMA was observed only in vascular endothelium (Figs. 5a–d).

Because control specimens were resected from patients with conjunctivochalasis, these samples were bulbar conjunctiva, whereas the samples from patients with VKC were palpebral conjunctiva. GPs are extremely rare in bulbar conjunctiva, so the fundamental anatomic differences between the two types of conjunctiva may have affected the results of this evaluation.

Stimulation of HConFs and STAT1 and STAT3 Phosphorylation by OSM

We performed immunocytochemistry to clarify whether HConFs have OSMRβ: cultured HConFs had fluorescent

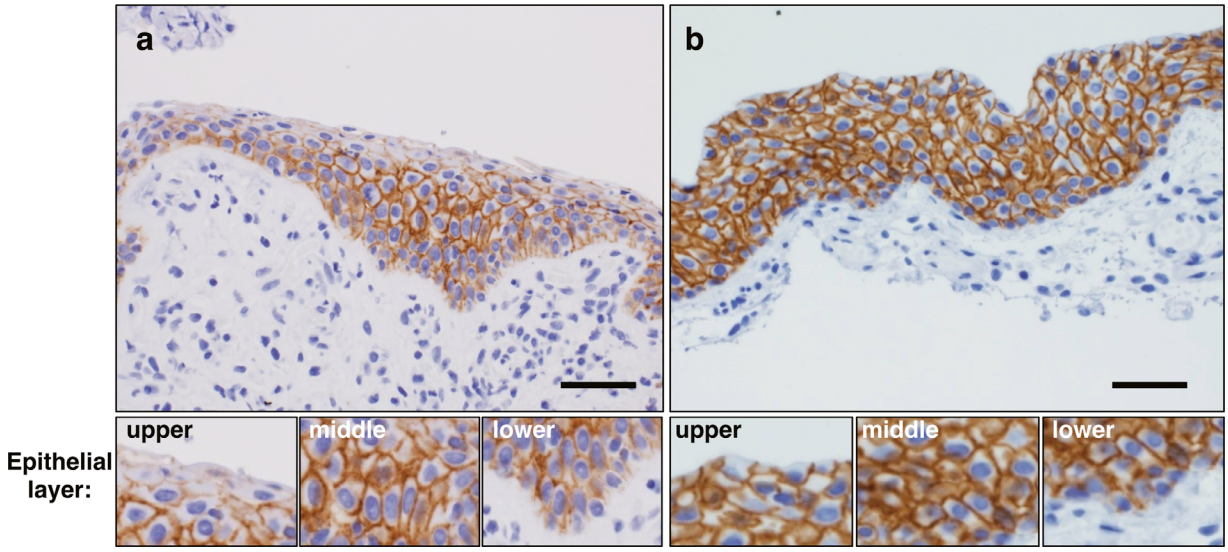

Figure 4. Expression of E-cadherin in giant papillae from patients with vernal keratoconjunctivitis and in control samples from patients with conjunctivochalasis. (**a**) Multilayer epithelium of giant papillae from patients with vernal keratoconjunctivitis. (**b**) Control samples (bulbar conjunctiva from patients with conjunctivochalasis). Immunoreactivity of E-cadherin appeared as a *brown* stain. Expansion images of each layer of epithelium (*lower figures*). *Bars*: 50 µm.

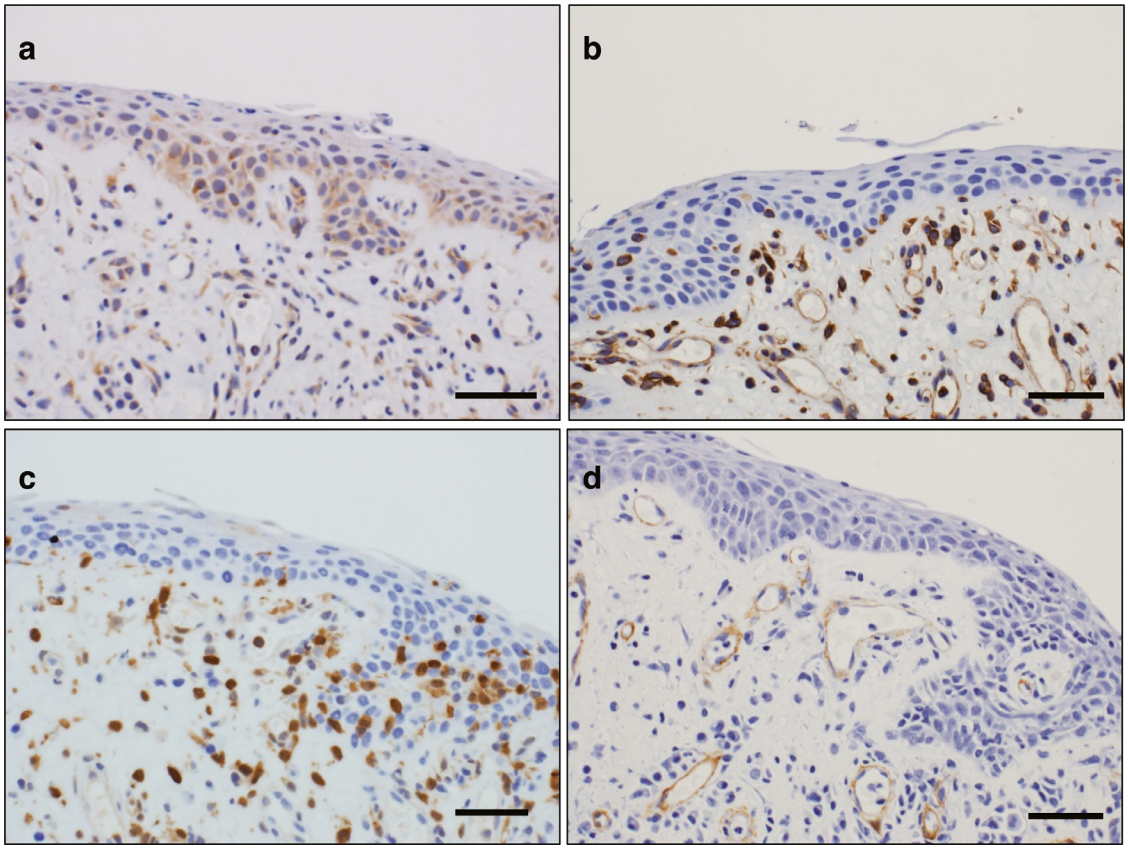

Figure 5. Expression of EMT-related proteins in the epithelium of giant papillae from patients with vernal keratoconjunctivitis. Expression of N-cadherin (**a**), vimentin (**b**), S100A4 (**c**), and α-SMA (**d**). Immunoreactivity of EMT-related proteins appeared as a *brown* stain. *Bars*: 50 µm.

Investigative Ophthalmology & Visual Science

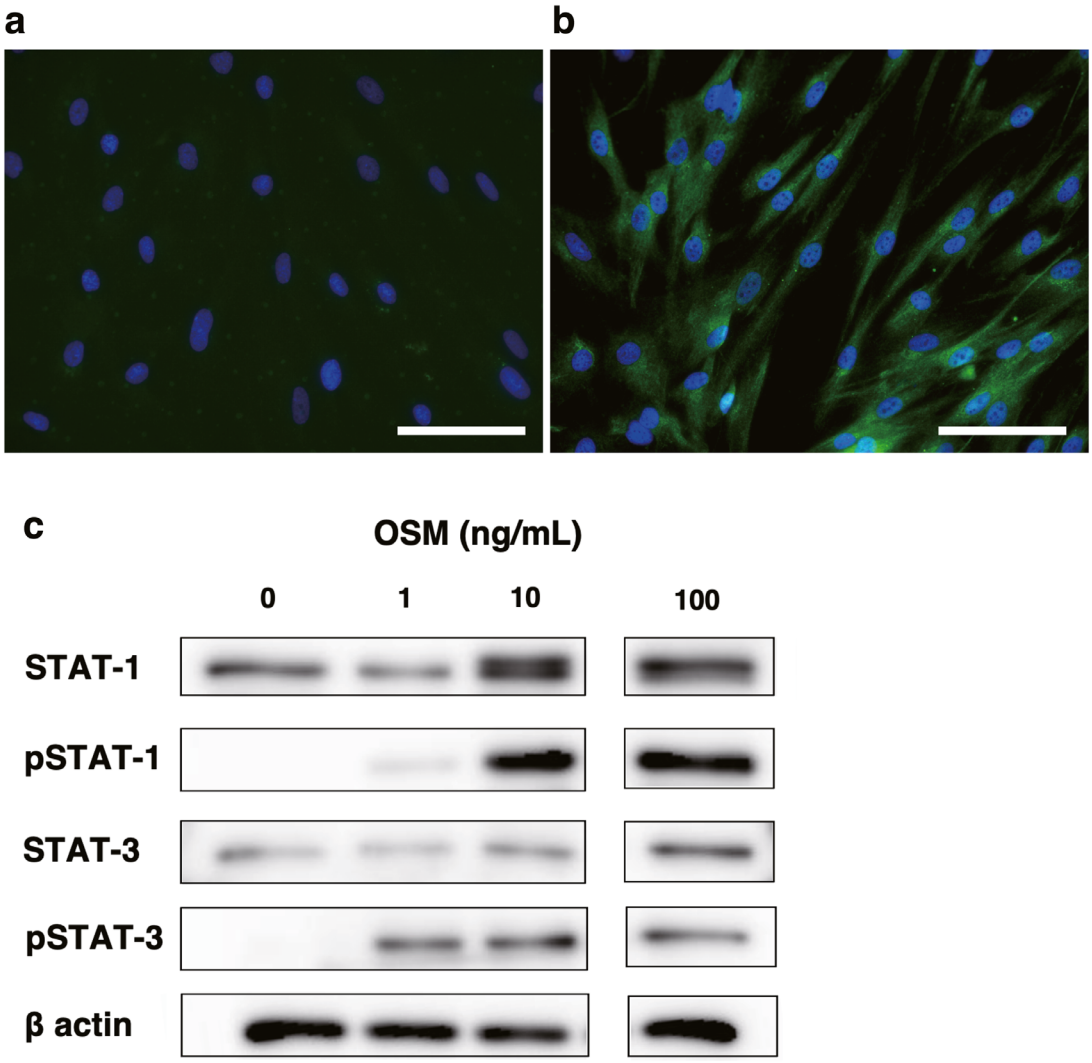

Figure 6. OSM-induced phosphorylation of signal transducer and activator of transcription 1 and 3 in human conjunctival fibroblasts. HConFs were stained with isotype control (**a**) or anti-OSM receptor β antibody (**b**). Immunoreactivity of OSMRβ appeared as a *green* stain. *Bars*: 10 µm. Expression of phosphorylated STAT1 and STAT3 in HConFs treated with OSM (0, 1, 10, and 100 ng/mL), assessed by Western blotting (**c**). Immunoreactive bands of β-actin (*lower row*) are shown as control.

signals for OSMRβ (Figs. 6a, 6b), showing that they could be stimulated by OSM. Next, to investigate whether OSM phosphorylates STAT1 and STAT3 in HConFs, we assessed expression of total STAT1 and STAT 3, pSTAT1, and pSTAT3 by Western blotting. Phosphorylation of STAT1 and STAT3 was not seen without OSM, but OSM treatment increased the level of pSTAT1 and pSTAT3 (Fig. 6c), revealing that OSM can activate the Janus kinase/STAT pathway in HConFs.

Global Gene Expression Analysis and ELISA in OSM-Treated HConFs

To investigate the effects of OSM in HConFs, global gene expression in OSM-treated or non-OSM-treated HConFs was analyzed by microarray. For this analysis, 148 genes (495 probes) in OSM-treated HConFs were upregulated 2-fold or more ($\log_2$ fold change >1) and 76 genes (453 probes) were downregulated 0.5-fold or less ($\log_2$ fold change <−1) (Figs. 7a, 7b). Several genes related to inflammation, fibrosis, or EMT, such as *SOCS3*, *SERPIN B3*, *IL-33*, *CCL8*, and *VEGF*, were mainly upregulated in OSM-treated HConFs.

Next, we assessed the expression change of these genes in OSM-treated HConFs by quantitative real-time PCR: the mRNA expressions of these molecules were increased in OSM-treated HConFs in a dose-dependent manner (Fig. 7c).

Finally, we investigated the protein expression of IL-33 in OSM-treated HConFs by ELISA and found that IL-33 was increased in cell lysate (Fig. 7d).

Expression of IL-33 in Conjunctival Fibroblasts in GPs

We performed immunohistochemical analysis to confirm the expression of IL-33 in VKC GPs. Double immunofluorescence of conjunctival fibroblasts and IL-33 antibodies showed positive IL-33 staining in the nucleus of fibroblasts (Figs. 8a–c).

Investigative Ophthalmology & Visual Science

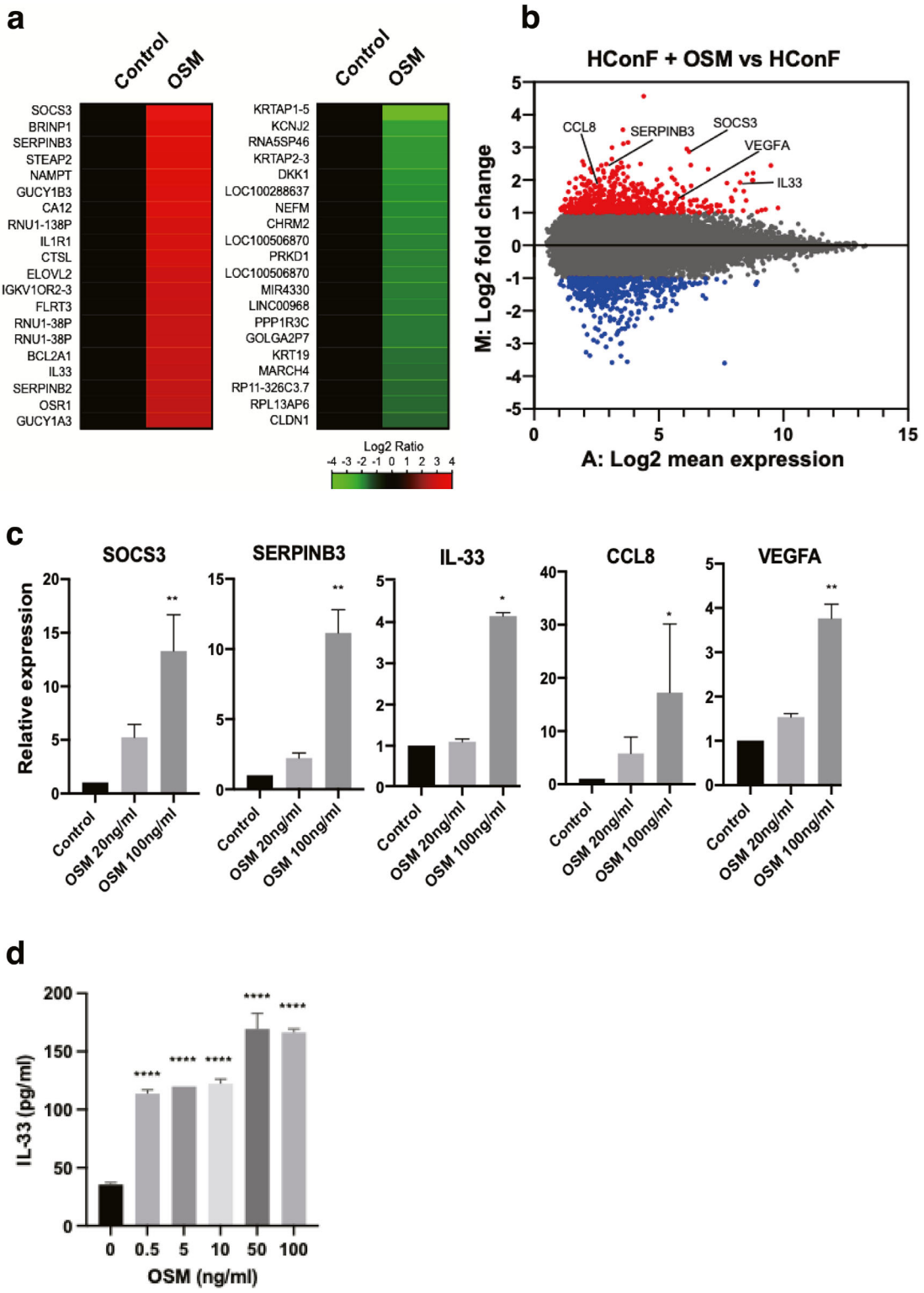

Figure 7. Effects of OSM on gene and protein expression in human conjunctival fibroblasts. (**a**) Heatmap showing the top 20 genes that were upregulated (*red scale*) or downregulated (*green scale*) in HConFs treated with OSM (100 ng/mL) (upregulated genes, 148 with >2-fold change; downregulated genes, 76 with <0.5-fold change). (**b**) MA plot of difference in gene expression between control vehicle samples and samples treated with OSM (100 ng/mL). (**c**) Expression levels of *SOCS3*, *SERPIN B3*, *IL-33*, *CCL8*, and *VEGF-A* in HConFs treated with OSM (0, 20, and 100 ng/mL), assessed by quantitative real-time PCR. *Error bars* show the SD (*$P < 0.05$, **$P < 0.01$, one-way ANOVA with Tukey test). (**d**) Protein levels of IL-33 in cell lysate of HConFs treated by OSM, assessed by enzyme-linked immunosorbent assay. *Error bars* show the SD (****$P < 0.0001$, one-way ANOVA with Tukey test).

Investigative Ophthalmology & Visual Science

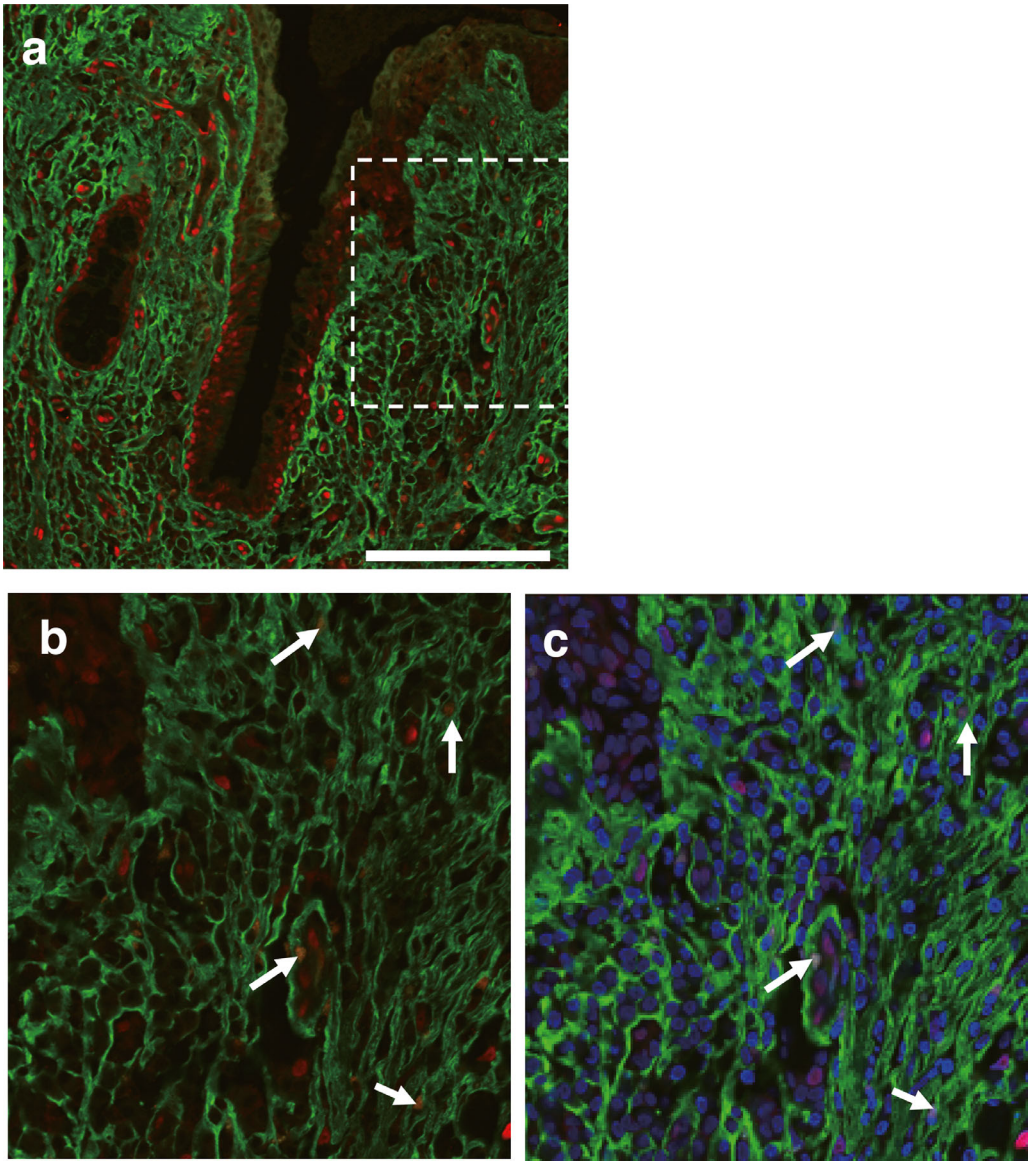

Figure 8. Expression of IL-33 by conjunctival fibroblasts in giant papillae from patients with vernal keratoconjunctivitis. (**a**) Anti–IL-33 antibody staining of the nucleus of conjunctival epithelial cells and fibroblasts (*red*) and anti–fibroblast antibody staining of the cytoplasm of fibroblasts (*green*). *Bar*: 200 µm. (**b**) Enlarged image of (**a**) showing conjunctival fibroblasts expressing IL-33 (*arrows*). (**c**) Same area as shown in (**b**), with 4′,6-diamidino-2-phenylindole staining.

Discussion

In this study, we observed some molecular expressions of VKC GPs and demonstrated that OSM impairs the barrier function of cultured HConEpiCs, as shown by TEER and an FITC-dextran permeability assay. We also showed by immunofluorescence and Western blotting that OSM decreases the expression of E-cadherin and ZO-1 in HConEpiCs. E-cadherin and ZO-1 were selected as examples of cell adhesion molecules that build the epithelial structure and barrier. Normally, E-cadherin is expressed along the cell membrane, where it is critical for the maintenance of epithelial barrier functions, such as tight junctions.

The mechanism of OSM-mediated barrier dysfunction in mucosal epithelium is currently unknown.[30] One hypothesis is that OSM directly downregulates expression of tight junction–related proteins.[30] Another is that OSM affects EMT (i.e., the transition from polarized epithelial cells to nonpolarized mesenchymal cells).[11–15,30] EMT requires downregulation of tight junction proteins, such as E-cadherin, ZO-1, and occludin, and upregulation of proteins important for maintenance of the mesenchymal phenotype, such as N-cadherin, vimentin, S100A4, and α-SMA. In this study, we rarely observed expression of these proteins in the epithelium of GPs; nevertheless, our findings do not necessarily indicate that EMT was not occurring: EMT is not binary phenomenon,[31] and our results were consistent with previous reports and may suggest partial EMT in VKC GPs. However, OSM did not induce expression of EMT-related proteins in cultured conjunctival epithelial cells and fibroblasts directly (data not shown). Further in vitro examinations are needed. The last hypothesis is that OSM induces epithelial cells to enter a chronically proliferative state in which tight junctions are not established.[30] E-cadherin is

Investigative Ophthalmology & Visual Science

a potent tumor suppressor because homophilic binding of E-cadherin inhibits cell proliferation, and it is often downregulated in malignant epithelial cancers. Immunohistologic analysis demonstrated that E-cadherin expression appeared in a cytoplasmic pattern, but not in a cell membrane pattern, in the lower epithelial layer of GPs. This result may reveal that OSM induces epithelial cells to a proliferation state in GPs. In addition, the expression of Ki-67, a marker of proliferation, was increased in the same epithelial layer. These findings indicate that there may be relationship between E-cadherin and cell proliferation in VKC in vivo.

The mechanism by which E-cadherin disappears in the upper epithelial layer of GPs is unknown; however, our previous study showed a high concentration of mast cell chymase in the tears of patients with VKC cleaved tight junction–related proteins.[32,33] Overall, the conjunctival epithelium of GPs seems to be structurally weaker and more permeable to allergens, allowing them to reach the substantia propria, where a lot of mast cells reside, and resulting in more pronounced allergic inflammation than in normal epithelium.

Next, we investigated the effects of OSM on conjunctival fibroblasts. OSM strongly activated STAT1 and STAT3 via OSMRβ and upregulated various genes related to allergic inflammation, such as *IL-33, VEGF*, and *CCL8*. Among these genes, *IL-33* may be important in allergic inflammation. The protein IL-33 belongs to the IL-1 family of cytokines, which may have broad effects that extend from early immune development to atopic disease exacerbations. IL-33 was identified as the ligand for suppression of tumorigenicity 2 (ST2), which is constitutively expressed on several immune cell types, including mast cells, innate lymphoid cells 2 (ILC2s), and T helper type 2 (Th2) cells. Among these cells, ILC2s have a crucial role in the innate allergic reaction. IL-33 is a particularly potent activator of ILC2s, which produce type 2 cytokines such as IL-13 and IL-5.[34–37] IL-33 binds to a heteromeric receptor consisting of ST2 and its coreceptor, IL-1 receptor accessory protein. Genetic studies have demonstrated reproducible, significant associations between IL-33/ST2 genetic variants and asthma in humans. Genetic variants in ST2 are also associated with atopic dermatitis risk,[38] and genetic variants in IL-33 and ST2 loci are associated with eosinophilic esophagitis risk.[39–42] In our previous studies, the expression of IL-33 was observed in the epithelium and vascular endothelial cells in VKC GPs.[26] A next-generation sequencer analysis study also showed that expression of the *IL-33* gene was among the top 20 highly expressed genes in GPs.[43] In a papain-driven mouse model of allergic conjunctival inflammation, IL-33–mediated activation of ILC2 played an important role in inducing eosinophils in conjunctival tissue.[44] These results may indicate that IL-33 has a crucial role in allergic inflammation in VKC.

Th2-driving cytokines such as IL-33, thymic stromal lymphopoietin, and IL-25 are control regulators of innate allergic inflammation. Although these molecules lack the signal sequence required for conventional secretory pathways, they can be released as an "alarmin" or as DAMPs in response to cellular injury or stress.[45,46] Epithelial cells and vascular endothelial cells, both of which express IL-33 constitutively in the nucleus, are thought to be the primary sources of IL-33 in inflammatory conditions.[25,47,48] However, in this study, immunohistologic analysis revealed that fibroblasts expressing IL-33 reside in GPs. In addition, OSM induced expression of IL-33 in cultured HConFs. Therefore, conjunctival fibroblasts stimulated by OSM may be another source of IL-33.

In conclusion, high levels of OSM may induce barrier dysfunction of the epithelium of VKC GPs and help antigens and OSM itself cross the epithelium. Furthermore, OSM may induce conjunctival fibroblasts to produce IL-33, a key molecule of innate type 2 responses. These effects indicate that OSM may have a crucial role in severe, prolonged allergic inflammation. In the future, maintenance of the barrier function of the conjunctival epithelium may be a treatment target in severe VKC.

Acknowledgments

Disclosure: **I. Ninomiya**, None; **K. Yamatoya**, None; **K. Mashimo**, None; **A. Matsuda**, None; **A. Usui-Ouchi**, None; **Y. Araki**, None; **N. Ebihara**, None

References

1. Tanaka M, Miyajima A. Oncostatin M, a multifunctional cytokine. *Rev Physiol Biochem Pharmacol.* 2003;149:39–52.
2. Boniface K, Diveu C, Morel F, et al. Oncostatin M secreted by skin infiltrating T lymphocytes is a potent keratinocyte activator involved in skin inflammation. *J Immunol.* 2007;178:4615–4622.
3. Suda T, Chida K, Todate A, et al. Oncostatin M production by human dendritic cells in response to bacterial products. *Cytokine.* 2002;17:335–340.
4. Salamon P, Shoham NG, Puxeddu I, et al. Human mast cells release oncostatin M on contact with activated T cells: possible biologic relevance. *J Allergy Clin Immunol.* 2008;121:448–455.
5. Grenier A, Dehoux M, Boutten A, et al. Oncostatin M production and regulation by human polymorphonuclear neutrophils. *Blood.* 1999;93:1413–1421.
6. Pothoven KL, Norton JE, Suh LA, et al. Neutrophils are a major source of the epithelial barrier disrupting cytokine oncostatin M in patients with mucosal airways disease. *J Allergy Clin Immunol.* 2017;139:1966–1978.
7. Nagahama KY, Togo S, Holz O, et al. Oncostatin M modulates fibroblast function via signal transducers and activators of transcription proteins-3. *Am J Respir Cell Mol Biol.* 2013;49:582–591.
8. Beigel F, Friedrich M, Probst C, et al. Oncostatin M mediates STAT3-dependent intestinal epithelial restitution via increased cell proliferation, decreased apoptosis and upregulation of SERPIN family members. *PLoS One.* 2014;9:e93498.
9. Jones SA, Jenkins BJ. Recent insights into targeting the IL-6 cytokine family in inflammatory diseases and cancer. *Nat Rev Immunol.* 2018;18:773–789.
10. Rabeony H, Petit-Paris I, Garnier J, et al. Inhibition of keratinocyte differentiation by the synergistic effect of IL-17A, IL-22, IL-1α, TNFα and oncostatin M. *PLoS One.* 2014;9:e101937.
11. Pollack V, Sarközi R, Banki Z, et al. Oncostatin M-induced effects on EMT in human proximal tubular cells: differential role of ERK signaling. *Am J Physiol Renal Physiol.* 2007;293:F1714–D1726.
12. Argast GM, Mercado P, Mulford IJ, et al. Cooperative signaling between oncostatin M, hepatocyte growth factor and transforming growth factor-β enhances epithelial to mesenchymal transition in lung and pancreatic tumor models. *Cells Tissues Organs.* 2011;193:114–132.
13. Guo L, Chen C, Shi M, et al. Stat3-coordinated Lin-28-let-7-HMGA2 and miR-200-ZEB1 circuits initiate and

maintain oncostatin M-driven epithelial-mesenchymal transition. *Oncogene*. 2013;32:5272–5282.
14. West NR, Murray JI, Watson PH. Oncostatin-M promotes phenotypic changes associated with mesenchymal and stem cell-like differentiation in breast cancer. *Oncogene*. 2014;33:1485–1494.
15. Nightingale J, Patel S, Suzuki N, et al. Oncostatin M, a cytokine released by activated mononuclear cells, induces epithelial cell-myofibroblast transdifferentiation via Jak/Stat pathway activation. *J Am Soc Nephrol*. 2004;15:21–32.
16. Mashimo K, Usui-Ouchi A, Ito Y, et al. Role of oncostatin M in the pathogenesis of vernal keratoconjunctivitis: focus on tissue remodeling. *Jpn J Ophthalmol*. 2021;65(1):144–153.
17. Takata F, Dohgu S, Matsumoto J, et al. Oncostatin M-induced blood-brain barrier impairment is due to prolonged activation of STAT3 signaling in vitro. *J Cell Biochem*. 2018;119:9055–9063.
18. Pothoven KL, Norton JE, Hulse KE, et al. Oncostatin M promotes mucosal epithelial barrier dysfunction, and its expression is increased in patients with eosinophilic mucosal disease. *J Allergy Clin Immunol*. 2015;136:737–746.
19. Takata F, Dohgu S, Sakaguchi S, et al. Oncostatin-M-reactive pericytes aggravate blood-brain barrier dysfunction by activating JAK/STAT3 signaling in vitro. *Neuroscience*. 2019;422:12–20.
20. Tan B, Luo W, Shen Z, et al. Roseburia intestinalis inhibits oncostatin M and maintains tight junction integrity in a murine model of acute experimental colitis. *Scand J Gastroenterol*. 2019;54:432–440.
21. Pothoven KL, Norton JE, Suh LA, et al. Neutrophils are a major source of the epithelial barrier disrupting cytokine oncostatin M in patients with mucosal airways disease. *J Allergy Clin Immunol*. 2017;139:1966–1978.
22. Fritz DK, Kerr C, Fattouh R, et al. A mouse model of airway disease: oncostatin M-induced pulmonary eosinophilia, goblet cell hyperplasia, and airway hyperresponsiveness are STAT6 dependent, and interstitial pulmonary fibrosis is STAT6 independent. *J Immunol*. 2011;186:1107–1118.
23. Kang HJ, Kang JS, Lee SH, et al. Upregulation of oncostatin M in allergic rhinitis. *Laryngoscope*. 2005;115:2213–2216.
24. Mozaffarian A, Brewer AW, Trueblood ES, et al. Mechanisms of oncostatin M-induced pulmonary inflammation and fibrosis. *J Immunol*. 2008;181:7243–7253.
25. Cayrol C, Girard JP. Interleukin-33 (IL-33): a nuclear cytokine from the IL-1 family. *Immunol Rev*. 2018;281:154–168.
26. Matsuda A, Okayama Y, Terai N, et al. The role of interleukin-33 in chronic allergic conjunctivitis. *Invest Ophthalmol Vis Sci* 2009;50:4646–4652.
27. Tanioka H, Kawasaki S, Yamasaki K, et al. Establishment of a cultivated human conjunctival epithelium as an alternative tissue source for autologous corneal epithelial transplantation. *Invest Ophthalmol Vis Sci*. 2006;47:3820–3827.
28. Ang LP, Tanioka H, Kawasaki S, et al. Cultivated human conjunctival epithelial transplantation for total limbal stem cell deficiency. *Invest Ophthalmol Vis Sci*. 2010;51:758–764.
29. Kinoshita S, Kawasaki S, Kitazawa K, et al. Establishment of a human conjunctival epithelial cell line lacking the functional TACSTD2 gene (an American Ophthalmological Society thesis). *Trans Am Ophthalmol Soc*. 2012;110:166–177.
30. Pothoven KL, Schleimer RP. The barrier hypothesis and Oncostatin M: restoration of epithelial barrier function as a novel therapeutic strategy for the treatment of type 2 inflammatory disease. *Tissue Barriers*. 2017;5:e1341367.
31. Pastushenko I, Blanpain C. EMT transition states during tumor progression and metastasis. *Trends Cell Biol*. 2019;29(3):212–226.
32. Ebihara N, Funaki T, Takai S, et al. Tear chymase in vernal keratoconjunctivitis. *Curr Eye Res*. 2004;28:417–420.
33. Ebihara N, Funaki T, Takai S, et al. Mast cell chymase decreases the barrier function and inhibits the migration of corneal epithelial cells. *Curr Eye Res*. 2005;30:1061–1069.
34. Moro K, Yamada T, Tanabe M, et al. Innate production of T(H)2 cytokines by adipose tissue-associated c-Kit(+) Sca-1(+) lymphoid cells. *Nature*. 2010;463:540–544.
35. Halim TYF, Rana BMJ, Walker JA, et al. Tissue-restricted adaptive type 2 immunity is orchestrated by expression of the costimulatory molecule OX40L on group 2 innate lymphoid cells. *Immunity*. 2018;48:1195–1207.
36. Salimi M, Barlow JL, Saunders SP, et al. A role for IL-25 and IL-33-driven type-2 innate lymphoid cells in atopic dermatitis. *J Exp Med*. 2013;210:2939–2950.
37. Neill DR, Wong SH, Bellosi A, et al. Nuocytes represent a new innate effector leukocyte that mediates type-2 immunity. *Nature*. 2010;464:1367–13670.
38. Shimizu M, Matsuda A, Yanagisawa K, et al. Functional SNPs in the distal promoter of the ST2 gene are associated with atopic dermatitis. *Hum Mol Genet*. 2005;14:2919–2927.
39. Moffatt MF, Gut IG, Demenais F, et al. A large-scale, consortium-based genomewide association study of asthma. Cookson WOCM; GABRIEL Consortium. *N Engl J Med*. 2010;363:1211–1221.
40. Grotenboer NS, Ketelaar ME, Koppelman GH, Nawijn MC. Decoding asthma: translating genetic variation in IL33 and IL1RL1 into disease pathophysiology. *J Allergy Clin Immunol*. 2013;131:856–865.
41. Savinko T, Matikainen S, Saarialho-Kere U, et al. IL-33 and ST2 in atopic dermatitis: expression profiles and modulation by triggering factors. *J Invest Dermatol*. 2012;132:1392–1400.
42. Kottyan LC, Davis BP, Sherrill JD, et al. Genome-wide association analysis of eosinophilic esophagitis provides insight into the tissue specificity of this allergic disease. *Nat Genet*. 2014;46:895–900.
43. Matsuda A, Asada Y, Suita N, et al. Transcriptome profiling of refractory atopic keratoconjunctivitis by RNA sequencing. *J Allergy Clin Immunol*. 2019;143:1610–1614.
44. Asada Y, Nakae S, Ishida W, et al. Roles of epithelial cell-derived type 2-initiating cytokines in experimental allergic conjunctivitis. *Invest Ophthalmol Vis Sci*. 2015;56:5194–5202.
45. Kouzaki H, Iijima K, Kobayashi T, O'Grady SM, Kita H. The danger signal, extracellular ATP, is a sensor for an airborne allergen and triggers IL-33 release and innate Th2-type responses. *J Immunol*. 2011;186:4375–4387.
46. Kakkar R, Hei H, Dobner S, Lee RT. Interleukin 33 as a mechanically responsive cytokine secreted by living cells. *J Biol Chem*. 2012;287:6941–6948.
47. Moussion C, Ortega N, Girard JP. The IL-1-like cytokine IL-33 is constitutively expressed in the nucleus of endothelial cells and epithelial cells in vivo: a novel 'alarmin'? *PLoS One*. 2008;3:e3331.
48. Pichery M, Mirey E, Mercier P, et al. Endogenous IL-33 is highly expressed in mouse epithelial barrier tissues, lymphoid organs, brain, embryos, and inflamed tissues: in situ analysis using a novel Il-33-LacZ gene trap reporter strain. *J Immunol*. 2012;188:3488–3495.

Investigative Ophthalmology & Visual Science